

# Characterization of GPS Carrier Phase Multipath

J.K. Ray

M.E. Cannon

*Department of Geomatics Engineering,  
University of Calgary, Alberta, Canada*

## BIOGRAPHIES

Jayanta Kumar Ray is a Ph.D. student in Geomatics Engineering at the University of Calgary. He received a B.E. and M.Tech. in Electronics Engineering from the Bangalore University and Indian Institute of Science, India, respectively. He has been involved in GPS research since 1992 in the area of GPS receiver hardware and software development, the integration of GPS with low cost sensors and the mitigation of multipath.

M. Elizabeth Cannon is Professor in Geomatics Engineering at the University of Calgary. She has been involved in GPS research and development since 1984, and has worked extensively on the integration of GPS and inertial navigation systems for various applications. Dr. Cannon is a Past President of the ION.

## ABSTRACT

GPS carrier phase measurements are affected by multipath signals that can significantly affect the quality of data used for static and kinematic positioning applications. It is generally difficult to characterize this multipath using field data whereby the exact sources of the errors cannot be easily isolated. In this paper, carrier phase multipath parameters are identified and their influences on measurements are investigated through a theoretical analysis. Multipath effects are analyzed from a geometrical perspective whereby GPS signals are assumed to propagate through the advancement of a plane wavefront on which the phase of the GPS signals is the same. The differential path delay of the reflected signal with respect to the direct signal is then calculated. A multipath simulation model is developed and described wherein the multipath parameters can be varied and their influences observed. These parameters include i) the reflection coefficient, ii) the antenna to reflector distance, iii) the azimuth and elevation of the reflected signal iv) the existence of multiple reflectors, and v) satellite dynamics. Multipath characteristics such as frequency, error envelope, spatial correlation, and signal to noise

ratio are studied by varying these parameters. Only the specular component is addressed in this paper as the diffused component is random in nature and difficult to model in a deterministic form.

## INTRODUCTION

GPS carrier phase multipath errors have assumed importance due to the high accuracy demands in a number of applications. The differential carrier phase measurement is invariably used in high precision applications like static and kinematic surveying and attitude determination (e.g. Axelrad et al., 1994). Most of the errors in the carrier phase measurements, such as atmospheric delays, orbital and clock errors are spatially correlated and generally cancel through the differencing process for short baselines. However, carrier phase multipath is a highly localized error which does not cancel through differencing and therefore has been identified as the major source of error in many high precision applications (Braasch, 1996).

Several techniques have been developed to counter carrier phase multipath either using improved receiver hardware (Townsend et al., 1995; Garin and Rousseau, 1997) or data processing techniques (Axelrad et al., 1994; Moelker, 1997; Ray et al., 1998). Townsend et al. (1995) used the MEDLL technique whereas Garin and Rousseau (1997) used the Advanced Strobe Correlator to reduce the effect of carrier phase multipath. Axelrad et al. (1994) and Sleewaegen (1997) have exploited the signal-to-noise (SNR) information from the receiver in post mission, along with the antenna gain patterns, to estimate multipath. Moelker (1997) used a direction finding algorithm (e.g. MUSIC) with a MEDLL receiver to counter multipath. Ray et al. (1998) used the spatial correlation of the multipath error between multiple closely-spaced antennas that can be used in real time at a reference station.

For successful isolation and mitigation of this error, it is important to understand the cause of the multipath and its

characteristics. Efforts were made by several researchers to characterize code multipath effects (Hagerman, 1973; van Nee, 1995; Braasch, 1996). Analysis of carrier lock loop behavior in the presence of multipath is given in Braasch (1996) and van Nee (1995). Georgiadou and Kleusberg (1988) have presented some of the general characteristics of carrier phase multipath and its dependencies on GPS L1 and L2 frequencies. However, a comprehensive analysis on the overall behavior of carrier phase multipath under different circumstances has not been done. This paper identifies parameters of concern for

carrier phase multipath and analyzes their impact from a geometrical perspective through simulation models.

### MULTIPATH FROM A GEOMETRICAL PERSPECTIVE

In Figure 1, a typical multipath scenario is shown whereby A1 to A5 are several antennas placed close-by in a multi-antenna system and the reflection from two sources to A1 is shown. The other four antennas will also be affected by the reflected signals in a similar way.

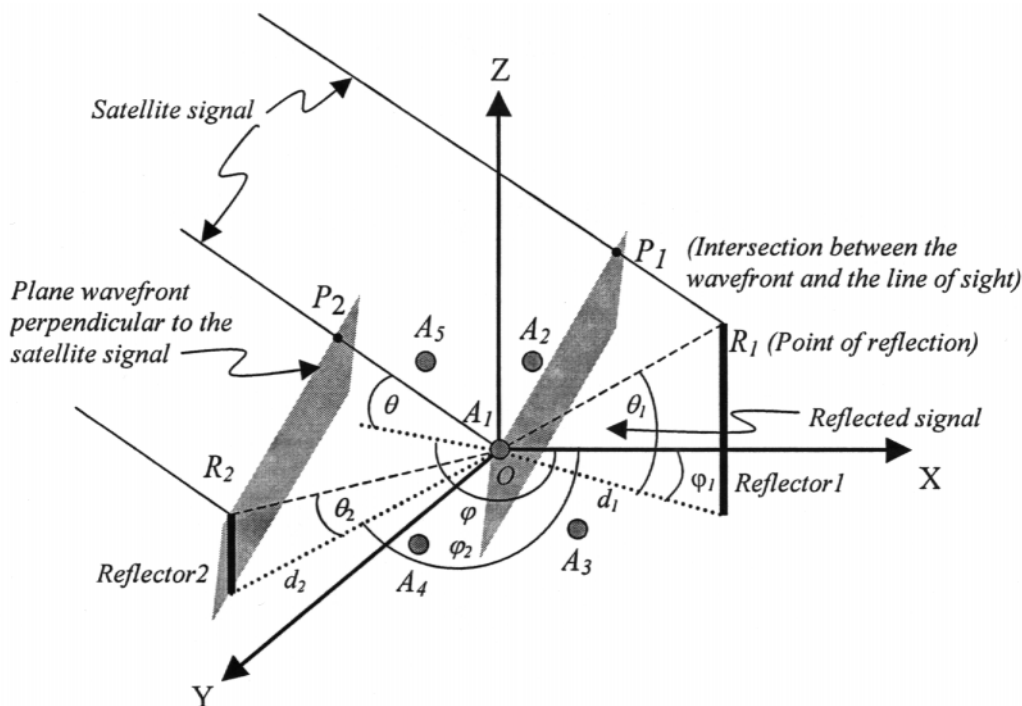


Figure 1: Direct and reflected signals to an antenna in a multi-antenna system

In the diagram,  $\theta$  and  $\varphi$  are the elevation and azimuth of the direct signal to the antenna while  $\theta_k$  and  $\varphi_k$  are the elevation and azimuth of the  $k$ th reflected signal to the antenna. The distance between the antenna and the reflector in the horizontal plane is denoted by  $d_k$ .

Two distinct scenarios are shown in the figure. In the first case (Reflector 1), the antenna (A1) is closer to the satellite compared to the reflector whereas in the second case (Reflector 2), the reflector is closer to the satellite compare to the antenna (A1). These two cases are generalized situations and representative of all the possible scenarios of the antenna-reflector geometry.

Since the satellite is 20,000 km above the earth, the GPS signal can be assumed to travel as parallel rays on the earth's surface. A plane wavefront perpendicular to the line of sight can be assumed to have the same carrier phase.

When this plane intersects the phase center of Antenna 1, it has the same carrier phase at all points on it, including point  $P_1$  (which is the intersection of the plane and the line of sight from Reflector 1 to the satellite). Therefore, the differential path delay of this reflected signal with respect to the direct signal is  $P_1R_1 + R_1O$ . The corresponding differential phase delay is computed by dividing the differential path delay by the signal wavelength.

Similarly, for case 2, a plane perpendicular to the line of sight from Reflector 2 to the satellite intersects the line of sight from the antenna under consideration at point  $P_2$ . In this case, the differential path delay is given by  $R_2O - P_2O$ .

Therefore, if the direct signal phase at the antenna is available, the reflected signal phase can be computed by adding the differential phase delay due to the differential path delay, to the direct signal phase.

In order to compute the effect of multipath on the direct signal, the above mentioned differential path delays need to be determined mathematically. By using solid geometry it can be shown that the differential path delay in either situations is given by,

$$a = d \left( \frac{1}{\cos \theta_k} - \tan \theta_k \sin \theta - \cos \theta \cos(\varphi - \varphi_k) \right). \quad (1)$$

In general, for several satellites in a multi-antenna system,

$$a_{jk}^i = d_{jk}^i \left( \begin{array}{l} \frac{1}{\cos(\theta_{jk}^i)} - \tan(\theta_{jk}^i) \sin(\theta_{j0}^i) \\ -\cos(\theta_{j0}^i) \cos(\varphi_{j0}^i - \varphi_{jk}^i) \end{array} \right) \quad (2)$$

where,

- $i$  is the satellite index
- $j$  is the antenna index
- $k$  is the reflected signal index;  $k = 0$  indicates the direct signal
- $a$  is the differential path delay of the reflected signal (m)
- $d$  is the horizontal distance between the antenna and the reflector (m)
- $\theta$  is the elevation of the direct satellite signal or the reflected signals (rad), and
- $\varphi$  is the azimuth of the direct satellite signal or the reflected signals (rad).

The differential path delay expression is a function of the satellite elevation and azimuth, the reflected signal elevation and azimuth and the antenna-reflector distance in the local level horizontal plane. This expression is further exploited to analyze the behavior of the carrier phase multipath error.

At the antenna phase center, the GPS signal consists of the direct as well as the reflected signals such that a receiver can not distinguish between them. In the receiver, multipath is characterized by four parameters, all of which are relative to the direct signal. These parameters are amplitude, path delay, phase and phase rate (Braasch, 1996).

The reflected signal amplitude depends upon several parameters, namely the reflection coefficient of the reflector material, the incident angle as well as the size of the reflector with respect to the first Fresnel zone (Beckmann and Spizzichino, 1963; Braasch, 1998).

The differential path delay of the reflected signal depends upon several parameters including the antenna reflector distance and geometry as shown in equation (2). The other two multipath parameters essentially depend upon the differential path delay and can be easily computed from it.

The relative phase is obtained directly by dividing the differential path delay by the signal wavelength and the phase rate is obtained by differentiating the phase. Therefore, equation (2) forms an important relationship that can be used to characterize the carrier phase multipath.

The composite signal at the antenna phase center, which consists of the direct and reflected signals is then given by,

$$s_j^i(t) = \sum_{k=0}^n D^i(t) C^i(t + \tau_{jk}^i) \alpha_{jk}^i S^i \cos \left( \begin{array}{l} \omega^i t + \phi_j^i \\ + \frac{2\pi a_{jk}^i}{\lambda_L} \end{array} \right) \quad (3)$$

where,

- $s$  is the composite signal to the antenna
- $D$  is the satellite data bit
- $C$  is the Pseudo Random Noise (PRN) code, i.e. either C/A or P code
- $S$  is the direct signal amplitude (v)
- $\tau$  is the differential time delay of the reflected signal (s)
- $\alpha$  is the reflection coefficient, defined by the ratio of direct signal amplitude to the reflected signal amplitude
- $\omega$  is the nominal carrier frequency (Hz)
- $t$  is the time (s)
- $\phi$  is the initial carrier phase (rad), and
- $\lambda_L$  is the carrier wavelength (m).

For simplicity, only one of the PRN code sequences and a noise-less situation is assumed in equation (3). Each of the direct and reflected signals consists of a carrier modulated by the code as well as a navigation data bit. The data bit is extracted in the receiver at a later stage and is of no concern as long as the correlation integration time in the receiver tracking loops is from data bit boundary to boundary. The PRN code is despread in the receiver by beating the incoming signal with a local replica of the PRN code in a Delay Lock Loop. The carrier is tracked in a Phase Lock Loop, generally a Costas loop (Ward, 1996), where the incoming signal is mixed with the inphase and quadrature phase components of a local carrier generated from a Numerically Controlled Oscillator (NCO). The carrier lock loop phase discriminator expression is given by,

$$\Psi_j^i = \arctan \left( \frac{\sum_{k=0}^n A(\tau_{jk}^i) \alpha_{jk}^i \sin(\psi_{jk}^i + \gamma_{jk}^i)}{\sum_{k=0}^n A(\tau_{jk}^i) \alpha_{jk}^i \cos(\psi_{jk}^i + \gamma_{jk}^i)} \right) \quad (4)$$

where,

$A$  is the correlation function. For a PRN code without band limitation it is defined as,

$$A(\tau) = 1 - \frac{|\tau|}{T}, \quad |\tau| \leq T$$

$$= 0, \quad |\tau| > T \quad (5)$$

where,

$T$  is the PRN code bit period

$\Psi$  is the measured phase difference between the composite signal carrier and the locally generated carrier (rad)

$\psi$  is the true phase difference between the direct signal carrier and the locally generated carrier (rad), and

$\gamma$  is the differential phase delay due to the differential path delay of the reflected signal and equal to  $\frac{2\pi a}{\lambda_L}$  (rad).

In a receiver, the phase measurement is generated by accumulating the phase of the NCO output. In a benign environment where there are no reflected signals, the incoming signal carrier is the same as the direct signal carrier. The NCO-generated local carrier locks onto the direct carrier very accurately, and as a result, the true phase difference between the incoming signal carrier and the locally generated carrier is nearly zero (actually zero mean) and the resulting phase measurement is very accurate. In the presence of multipath, the composite signal phase shifts from the direct signal phase and the NCO-generated local carrier locks onto the composite carrier phase resulting in an error in the phase measurement. This error is equal to the difference between the composite signal carrier phase and the direct signal carrier phase.

It can be easily seen from the equation that when multipath is absent,

$$\alpha_{jk}^i = 0, \text{ for } k = 1, 2, \dots; \text{ then,}$$

$$\Psi_j^i = \psi_{j0}^i.$$

Under these circumstances, the measured phase is the correct phase when assuming no phase noise.

The error in the measured carrier phase is then calculated by,

$$\Delta\Psi_j^i = \Psi_j^i - \psi_j^i.$$

Using equation (4) it can be easily shown that,

$$\Delta\Psi_j^i = \arctan \left( \frac{\sum_{k=0}^n A(\tau_{jk}^i) \alpha_{jk}^i \sin(\gamma_{jk}^i)}{1 + \sum_{k=0}^n A(\tau_{jk}^i) \alpha_{jk}^i \cos(\gamma_{jk}^i)} \right). \quad (6)$$

If there is only one dominant reflector, the above equation reduces to,

$$\Delta\Psi_j^i = \arctan \left( \frac{A(\tau_{jl}^i) \alpha_{jl}^i \sin \gamma_{jl}^i}{1 + A(\tau_{jl}^i) \alpha_{jl}^i \cos \gamma_{jl}^i} \right). \quad (7)$$

From equation (7), it can be observed that the multipath error amplitude (in radians) is a function of the PRN code correlation function and the reflection coefficient, and independent of the carrier wavelength. This means that the L1 and L2 carriers will have the same amplitude of multipath error (in radians). The amplitude is also a function of the antenna-reflector distance through the correlation function. If the reflector is far away from the antenna (i.e.  $\tau$  is large), the correlation value decreases and so does the multipath error amplitude. As the distance approaches the PRN code chip, the correlation value as well as the multipath error diminish.

The multipath error phase is directly related to the relative phase of the reflected signal. Multipath error phase variation is due to the variation of the reflected signal relative phase or differential path delay. For the same differential path delay, GPS L1 and L2 signals will have different relative phase delays and correspondingly different phases of the multipath error. The rate of change of the phase or frequency of the multipath error may also be determined from this equation. This is also obtained by taking the time derivative of the differential path delay expression. Expressing the derivative in terms of phase rate rather than distant rate from equation (2), we get,

$$\frac{\delta\gamma_{jl}^i}{\delta t} = \frac{2\pi d_{jl}^i}{\lambda_L} \left( \begin{array}{l} \left\{ \sin \theta_j^i \cos(\phi_j^i - \phi_{jl}^i) \right\} \frac{\delta\theta_j^i}{\delta t} \\ - \cos \theta_j^i \tan \theta_{jl}^i \\ + \left\{ \cos \theta_j^i \sin(\phi_j^i - \phi_{jl}^i) \right\} \frac{\delta\phi_j^i}{\delta t} \end{array} \right). \quad (8)$$

The above expression is obtained under the assumption that the antenna-reflector geometry does not change significantly over the period under consideration. This assumption does not generally hold for kinematic receivers, where the antenna-reflector geometry may change rapidly. In stationary situations, if the geometry changes significantly, the partial derivatives with respect to the reflected signal elevation and azimuth are to be added in the above equation.

It is evident from equation (8) that the multipath error frequency is,

- directly proportional to the distance between the antenna and the reflector
- inversely proportional to the wavelength of the carrier signal
- directly proportional to the rate of change of elevation of the satellite
- directly proportional to the rate of change of azimuth of the satellite, and
- dependent upon the antenna-reflector and the line-of-sight vectors.

The above statements allow an analysis of the carrier phase multipath characteristics as follows,

- reflectors which are far away from an antenna cause high frequency or fast-changing multipath and close-by reflectors cause low frequency or slowly changing multipath
- GPS L1 and L2 carriers will have the same multipath amplitude but different instantaneous phases. The L1 carrier has higher frequency multipath compared to the L2 carrier
- reflectors which are far away from an antenna cause a weak multipath error compared to their close-by counterparts, and
- a low elevation satellite is more likely to cause carrier phase multipath (due to more potential reflectors) but requires a larger surface (due to the large Fresnel zone) for strong multipath. On the other hand, a high elevation satellite is less likely to cause carrier phase multipath but requires a smaller surface for strong multipath (Braasch, 1998).

## MULTIPATH AND SNR

GPS signal power or SNR is related to the carrier phase multipath parameters. It is to be emphasized that the code and data bit in the GPS signal do not contribute to the signal power as they merely change the phase of the carrier depending upon the modulation technique employed. The carrier or signal power with or without the data and code bits remains the same. Therefore, the receiver determines the power of the carrier, not code and data, and generally expresses it as the ratio of average signal power to noise power spectral density or  $C/N_0$  (Spilker Jr, 1996).

GPS signal power can therefore be determined from the composite signal in equation (3) by ignoring the code and data bit as follows,

$$s_j^i = S^i \sum_{k=0}^n \alpha_{jk}^i \cos(\omega^i t + \phi_j^i + \gamma_{jk}^i). \quad (9)$$

For a single dominant reflector, the equation simplifies to,

$$s_j^i = S^i \cos(\omega t + \phi_j^i) + S^i \alpha_{jl}^i \cos(\omega^i t + \phi_j^i + \gamma_{jl}^i). \quad (10)$$

Assuming a uniform antenna gain pattern, the average received signal power can be easily calculated from the above expression and is given by (Close, 1966),

$$P_j^i = P_{j0}^i \left( 1 + (\alpha_{jl}^i)^2 + 2\alpha_{jl}^i \cos(\gamma_{jl}^i) \right) \quad (11)$$

where,

$P_{j0}^i$  is the average power of the direct carrier signal

$$\text{and is equal to } \frac{(S^i)^2}{2}.$$

From equation (11), the total signal power in the receiver is a function of the reflection coefficient and relative phase of the reflected signal.

The maximum and minimum signal power may be obtained from equation (11) as,

$$P_j^i \Big|_{\max} = P_{j0}^i \left( 1 + \alpha_{jl}^i \right)^2, \quad \text{and} \quad (12)$$

$$P_j^i \Big|_{\min} = P_{j0}^i \left( 1 - \alpha_{jl}^i \right)^2. \quad (13)$$

Their ratio is

$$\frac{P_j^i \Big|_{\max}}{P_j^i \Big|_{\min}} = \frac{\left( 1 + \alpha_{jl}^i \right)^2}{\left( 1 - \alpha_{jl}^i \right)^2} = \frac{10^{\left( \frac{(C/N_0)_{\max}}{20} \right)}}{10^{\left( \frac{(C/N_0)_{\min}}{20} \right)}} = R. \quad (14)$$

Therefore,

$$\alpha_{jl}^i = \frac{\sqrt{R} - 1}{\sqrt{R} + 1}. \quad (15)$$

Equation (15) relates the reflection coefficient to the SNR, which means that the reflection coefficient may be estimated from the maximum and minimum SNR of the GPS signal in the receiver. These relationships may be used to estimate the reflection parameters from the SNR.

## SIMULATION DESCRIPTION

A carrier phase Multipath Simulation and Mitigation software (MultiSiM) for GPS system was developed on a PC platform. The major inputs to the simulator are,

- reflector parameters, and
- antenna parameters

while the major outputs from the simulator are,

- true carrier phase
- measured carrier phase contaminated with multipath and phase noise, and
- estimated carrier phase.

The software consists of two main modules namely, Simulation and Mitigation. The first module allows the user to define the multipath environment and the antenna setup through the input parameters. The user can input the number of reflectors per satellite and their locations with respect to the reference antenna position in order to simulate a controlled multipath environment. The user can also configure the antenna setup, i.e. the number of antennas and their placement.

The carrier phase of the direct and reflected signals at each antenna may be determined by computing the distance traveled by the signal up to the antenna. For the direct signal, it is the distance between the satellite and the antenna; while for the reflected signals it is the total distance from the satellite to the reflector plus the reflector to the antenna. The satellite position is determined from stored ephemeris data.

The measured carrier phase without noise contains two parts – the integer and fractional cycle components. Assuming that the direct signal is stronger than the indirect signal, the integer cycles in the measured carrier phase is same as the direct signal's integer cycles. The phase of the fractional cycle of the reflected signal is what actually corrupts the phase of the fractional cycle of the direct signal, depending upon its relative strength and phase. A single observation from the direct and all the reflected signals are generated per satellite-antenna combination. Gaussian noise with selected characteristics is added to the measurement.

## SIMULATION RESULTS

Figures 2(a) to 2(e) show the effect of a reflected signal on a direct signal for three different situations. In Figure 2(a), the direct signal modulated by the code and data is shown. There are many L1 carrier cycles within a code bit, and only a small fraction of it is illustrated to

demonstrate the behavior. Figure 2(b) is the reflected signal delayed by two integer cycles. It is also 90 degrees out of phase with respect to the direct signal and one half its amplitude. Figures 2(c), 2(d) and 2(e) show the composite signals consisting of a direct and reflected signal for a relative reflected signal phase of 90, 0 and 180 degrees, respectively. It is observed that in the first case, the composite signal has a phase error, but no change in amplitude. In contrast, in the second and third cases, the composite signals do not exhibit phase error, but the signal amplitude is increased and decreased respectively. This will affect the SNR or the more widely used  $C/N_0$  of the carrier. For a large out of phase reflected signal, the receiver may lose lock of the incoming signal.

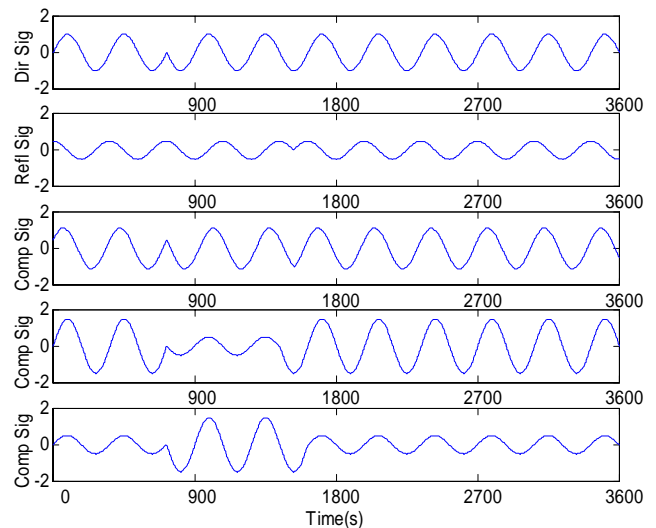


Figure 2(a-e): Waveforms of the direct, reflected and composite signals for 90, 0 and 180 degrees relative phase of the reflected signal from a reflector with a reflection coefficient of 0.5.

Figure 3(a) plots the multipath error against the differential path delay for a reflector with a reflection coefficient 0.9. It can be seen from equation (6) that the multipath error is a function of the correlation function. As the differential path delay increases, the correlation value of the reflected signal code with the locally generated replica decreases, thereby reducing multipath error. For a reflected signal delayed by more than one PRN code chip, the correlation value is zero (ignoring the correlation sidelobes) and so is the multipath error. Therefore for C/A and P code receivers, a differential path delay of more than 293.26 m and 29.33 m respectively do not contribute to multipath errors in the carrier phase measurements. Also, it can be noted that carrier phase multipath has a zero mean.

Figure 3(b) plots the multipath error envelope against the differential path delay for various reflection coefficients of the reflector. Multipath error is plotted in units of cycle

length and distance in units of code chips. Therefore, this figure is representative for multipath on an L1 as well as L2 carrier in a C/A or P code receiver. As expected, the multipath error envelope reduces for weaker reflected signals.

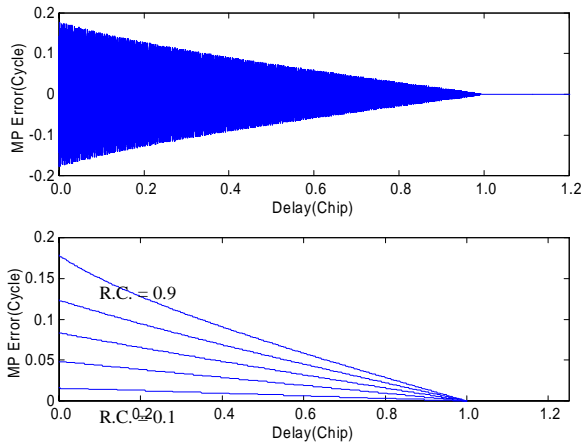


Figure 3(a-b): Multipath error vs. reflected signal path delay for a reflection coefficient of 0.9 and multipath error envelopes for reflection coefficients 0.1, 0.3, 0.5, 0.7 and 0.9.

Figures 4(a) to 4(c) demonstrate the variation of the multipath error as a function of satellite elevation and azimuth for satellite 4. Figure 4(c) is plotted using equation (7) for a reflector with reflection coefficient of 0.5 at a distance of 20 m from the antenna. A nominal phase noise of 3 mm ( $1\sigma$ ) is added. Though in practice, it is unlikely to have reflection from the same point for a long period, in this case it serves the purpose of understanding the general behavior of multipath error over time. In the figure, the multipath phase rate changes substantially depending upon the change in satellite azimuth and elevation.

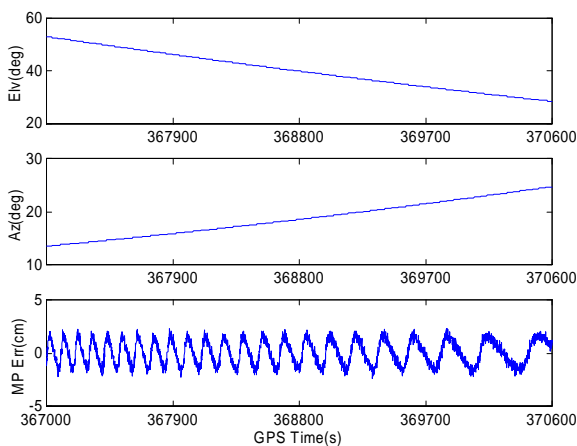


Figure 4(a-c): Multipath error variation as a function of elevation and azimuth for satellite 4 due to a reflector with reflection coefficient of 0.5 at a distance of 20 m from the antenna.

Figures 5(a) to 5(d) are generated under similar circumstances as in Figure 4(c) except that the reflector is now placed 5 m away from the antenna. In figures 5(b) and 5(c), the reflection coefficient is changed to 0.95 and 0.3, respectively. In figure 5(d), the reflector is placed in a different location but at the same distance with respect to the antenna. These figures show several important characteristics of multipath. It is clear from the figures that in a weak multipath situation, the error tends to be sinusoidal whereby the maxima and the minima are uniformly spaced at 90 and 270 degrees relative phase of the reflected signal. In a strong multipath situation however, the error tends to be an inverted sawtooth with sharp transitions in the vicinity of 180 degrees relative phase of the reflected signal. Also, the multipath phase and frequency is highly dependent on the location of the reflector. In fact, a small change in location, in the order of several cm, may change the differential path delay thereby causing a change in the reflected signal relative phase and multipath error. This makes the day to day prediction of carrier phase multipath highly vulnerable unless the environment is exactly the same. Furthermore, code multipath phase depends upon reflected signal relative phase and that makes code multipath error day to day prediction vulnerable as well.

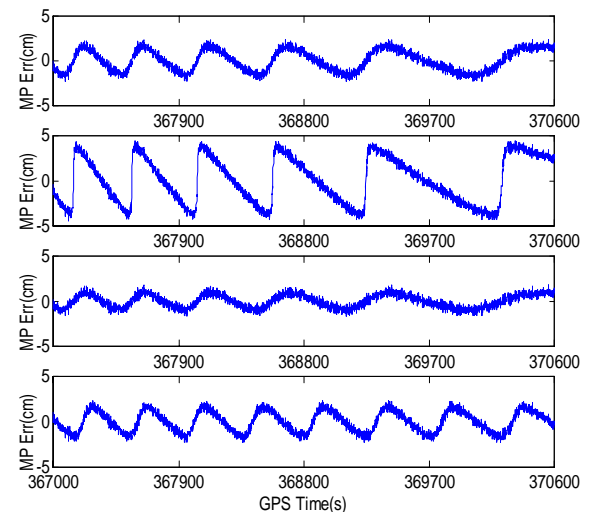


Figure 5(a-d): Multipath error for satellite 4 due to a single reflector with reflection coefficients of 0.5, 0.95, 0.3 and 0.5 respectively at a distance of 5 m from the antenna. For 5(d), the reflector is at different location.

Figures 6(a) to 6(d) display multipath errors from a large reflector at various closely-spaced antennas. It is clear from the figure that the multipath error is highly correlated between antennas. They have different phases due to different differential path delays of the reflected signal. Their correlation can be exploited to estimate the multipath error at individual antennas from single difference carrier phase measurements between antennas as demonstrated by Ray et al. (1998).

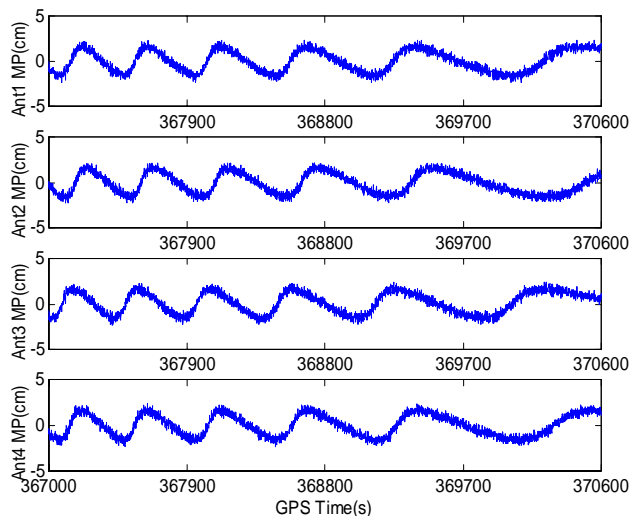


Figure 6(a-d): Multipath error at multiple antennas separated by 5 to 10 cm.

Figure 7(a) displays the multipath error due to an additional reflector compared to the set up used to generate data for Figures 5(a) and 6(a) to 6(d). It demonstrates the error behavior for both L1 and L2 carriers for satellite 4. Figure 7(b) shows the error behavior for satellite 16 due to the same reflectors. In these figures, the darker shaded error corresponds to the L1 carrier. Several important observations can be made from them: i) the multipath error may change substantially due to the addition or subtraction of another reflector, ii) the same set of reflectors have a different effect for various satellites depending upon the line-of-sight vector, antenna-reflector vector, elevation and azimuth of the satellite, iii) the multipath error has the same amplitude (in radians) for the L1 and L2 carrier, iv) the multipath error has a different phase for the L1 and L2 carrier. At a particular instant the multipath error for the L1 and L2 carriers look arbitrary, but over time the error signals have the same shape. The multipath error dependency on frequency is exploited by Georgiadou and Kleusberg (1988).

Figures 8(a) and 8(c) show the multipath error for satellite 4 and 16, respectively while Figures 8(b) and 8(d) are their estimated periods. Periods are estimated not from the error themselves, but from the antenna-reflector geometry using equation (8). Comparing the errors with their estimated periods, it is seen that the estimation is approximately correct for the entire duration. In the figures, estimation is based on the known position of the reflector, which is not available in practical applications. However, this relationship may be used to estimate the multipath error from the available measurements. For example, one can assume the reflector position and reflection coefficient to be the unknown state variables and then estimate them using measurements from the closely-spaced antennas.

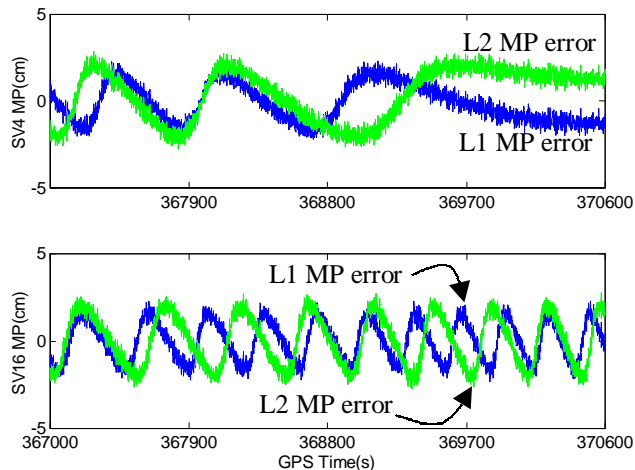


Figure 7(a-b): L1 and L2 multipath errors due to two reflectors for satellites 4 and 16, respectively.

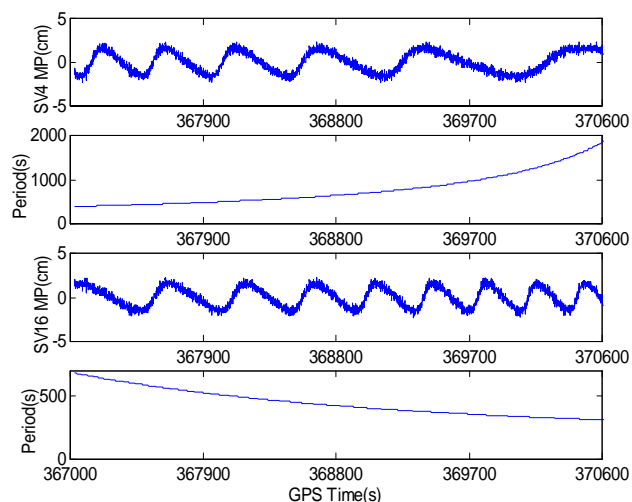


Figure 8(a-d): Multipath errors and their estimated periods for satellites 4 and 16.

Figure 9(a) shows the multipath error for the same setup used to generate the data for Figure 8(a) except that the reflection coefficient is changed to 0.3. Figure 9(b) is the ratio of the average composite signal power to the noise spectral density generated using equation (11). Similarly Figures 9(c) and 9(d) are the multipath error and the SNR due to a reflector with reflection coefficient 0.9. The nominal value of  $C/N_0$  due to the direct signal alone is 45 dB-Hz. It is clear from the plots that multipath error and SNR have distinct relationships. This is because the composite signal power and multipath error depend upon the relative phase of the reflected signal. For a small reflection coefficient, the multipath error is at an absolute maximum at 90 and 270 degrees and is zero at 0 and 180 degrees of the reflected signal relative phase (Figure 9(a)). However, for a high reflection coefficient, multipath error is at absolute maximum value at the vicinity of 180 degrees of the reflected signal relative

phase (Figure 9(c)). In contrast, the carrier power is maximum and minimum at 0 and 180 degrees respectively of the reflected signal relative phase for all reflection coefficients. Also from figure 9(b), the maximum and minimum power is approximately 49.5 and 39 dB-Hz. Using equations (14) and (15) the estimated reflection coefficient is approximately 0.3, which is correct. The relationship between the SNR and multipath error is exploited by researchers to estimate carrier phase multipath (Axelrad et al., 1994; Sleewaegen, 1997).

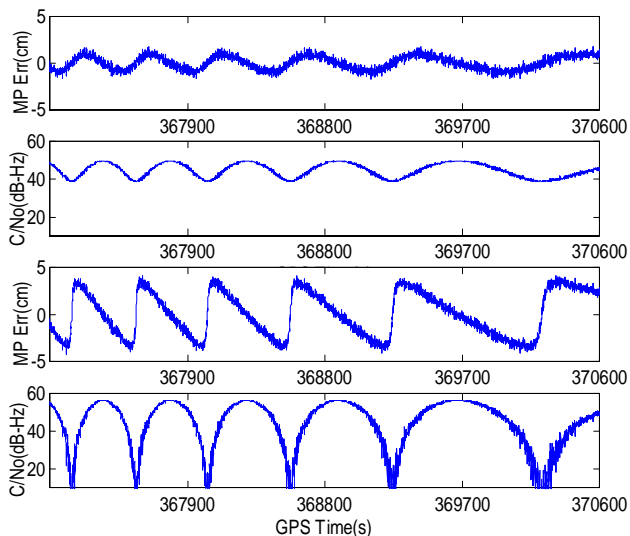


Figure 9(a-d): Multipath error and SNR for satellite 4 due to a reflector with reflection coefficient of 0.3 and 0.9 at a distance of 5 m from the antenna.

## CONCLUSIONS

Carrier phase multipath is a major source of error for high accuracy differential carrier phase positioning. Effective multipath mitigation techniques or multipath avoidance requires a sound understanding of its characteristics. In this paper, various parameters of the carrier phase multipath are analyzed from theoretical and simulation models. The problem is approached from a geometrical perspective and exploits the antenna-reflector geometry to characterize multipath.

Major findings of this work are the computation of the various relationships between such parameters as the multipath amplitude, phase and frequency with the satellite dynamics, antenna-reflector distance, antenna-reflector geometry, signal frequency, and SNR. The analysis is also extended for multiple reflectors and multiple closely-spaced antennas.

This analysis may be further extended using image theory of electromagnetic signals. The extent of the change in signal polarization due to reflection, and its effect on

various antennas, requires further research. A comprehensive comparison of code multipath and carrier phase multipath is yet to be compiled. Furthermore, simulations need to be substantiated through real data analysis to confirm the findings.

## REFERENCES

- Axelrad, P., C. Comp, and P. MacDoran, (1994), Use of Signal-To-Noise Ratio for Multipath Error Correction in GPS Differential Phase Measurements: Methodology and Experimental Results, Proceedings of ION GPS-94, Salt Lake City, September 20-23, pp. 655-666.
- Backer, D., K.H.Thiel, and P.Hartl (1994), A special Method of Managing Multipath Effects, Proceedings of ION GPS-94, Salt Lake City, September 20-23, pp. 157-163.
- Beckmann, P. and A. Spizzichino (1963), The scattering of Electromagnetic Waves from Rough Surfaces, Pergamon Press, 503 pp.
- Braasch, M.S. and F. van Graas (1991), Guidance Accuracy Considerations for Realtime GPS Interferometry, Proceedings of ION GPS-91, Albuquerque, September 9-13, pp. 373-386.
- Braasch, M.S. (1996), Multipath Effects, Global Positioning Systems: Theory and Applications, American Institute of Aeronautics and Astronautics, Vol. 1, Chapter 14, pp. 547-568.
- Braasch M. S. (1998), Viewgraphs of the lecture presented at the University of Calgary, July 8, 73 pp.
- Breeuwer, E. (1992), Modeling and Measuring GPS Multipath Effects, Master's Thesis, Faculty of Electrical Engineering, Delft University of Technology, Delft, The Netherlands, January 1992. 117 pp.
- Cannon, M.E. and G. Lachapelle (1992), Analysis of a High-Performance C/A-Code GPS Receiver in Kinematic Mode, NAVIGATION: Journal of The Institute of Navigation, Vol. 39, No. 3, Fall, pp. 285-300.
- Cannon, M.E. and J. Shi (1995), Precise Airborne Carrier Phase-based GPS Positioning with a Multi-Receiver Configuration: Data Processing and Accuracy Evaluation, Canadian Aeronautics and Space Journal, Vol. 41, No. 1, March, pp. 40-48.

- Close, C.M. (1966), The Analysis of Linear Circuits, Harcourt, Brace & World, Inc., 716 pp.
- Dixon, R.C. (1976), Spread Spectrum Techniques, IEEE Press, New York, 422 pp.
- Garin L and J. Rousseau (1997), Enhanced Strobe Correlator Multipath Rejection for Code & Carrier, Proceedings of ION GPS-97, September 16-19, Kansas City, pp. 559-568.
- GP2021 Data Sheet (1996), GPS 12 Channel Correlator with Microprocessor Support Functions, GEC Plessey Semiconductors, July, 64 pp.
- Georgiadou, Y and A. Kleusberg (1988), On Carrier Signal Multipath Effects in relative GPS Positioning, manuscripta geodatica, Springer-Verlag, Vol. 13, No. 3, pp. 172-179.
- Hagerman, L.L. (1973), Effects of Multipath on Coherent and Non-coherent PRN Ranging Receiver, Aerospace Report No. TOR-0073 (3020 – 03) –3, Development Planning Division, The Aerospace Corporation, 39 pp.
- Jordan, E.C. and K.G. Balmain (1972), Electromagnetic Waves and Radiating Systems, Second Edition, Prentice-Hall, Inc. 753 pp.
- Lachapelle, G., W. Falkenberg, D. Neufeldt and P. Keilland (1989), Marine DGPS Using Code and Carrier in Multipath Environment, Proceedings of ION GPS-89, Colorado Springs, September 27-29, pp. 343-347.
- Lachapelle, G. (1997), Lecture notes of GPS Theory and applications, The University of Calgary, Fall 1997, 444 pp.
- Moelker, D. (1997), Multiple Antennas for Advanced GNSS Multipath Mitigation and Multipath Direction Finding, Proceedings of ION GPS-97, September 16-19, Kansas City, pp. 541-550.
- Ray, J.K., M.E. Cannon and P. Fenton (1998), Mitigation of Static Carrier Phase Multipath Effects Using Multiple Closely-Spaced Antennas, Proceedings of ION GPS-98, Nashville, September 15-18 (in press).
- Sleewaegen, J. (1997), Multipath Mitigation, Benefits from using the Signal-to-Noise Ratio, Proceedings of ION GPS-97, Kansas City, September 16-19, pp. 531-540.
- Spilker Jr., J. J. (1980), GPS Signal Structure and Performance Characteristics, Global Positioning Systems (Red book), The Institute of Navigation, Vol. 1, pp. 29-54.
- Spilker Jr., J. J. (1996), GPS Signal Structure and Theoretical Performance, Global Positioning Systems: Theory and Applications, American Institute of Aeronautics and Astronautics, Vol. 1, Chapter 3, pp. 57-120.
- Townsend, B., P. Fenton, K.van Dierendonck and R.D.J. van Nee (1995), L1 Carrier Phase Multipath Error Reduction Using MEDLL Technology, Proceedings of ION GPS-95, Palm Spring, September 12-15, pp. 1539-1544.
- Tranquilla, J. and J. Carr (1990-91), GPS Multipath Field Observations at Land and Water Sites, NAVIGATION: Journal of the Institute of Navigation, Vol. 37, No. 4, Winter, pp. 393-414.
- van Nee, R.D.J. (1995), Multipath and Multi-Transmitter Interference in Spread-Spectrum Communication and Navigation Systems, Delft University Press, Delft, The Netherlands, 208 pp.
- Ward P. (1996), Satellite Signal Acquisition and Tracking, Understanding GPS Principles and Applications, Artech House, Chapter 5, pp. 119-208.
- Weill, L.R. (1997), Conquering Multipath: The GPS Accuracy Battle, Innovation, GPS World, Vol. 8, No. 4, April 1997, pp. 59-66.